Antiviral Research 182 (2020) 104924

Contents lists available at ScienceDirect

Antiviral Research

journal homepage: www.elsevier.com/locate/antiviral

Research paper

Evaluation of SARS-CoV-2 3C-like protease inhibitors using self-assembled monolayer desorption ionization mass spectrometry

Zachary A. Gurard-Levin [a], Cheng Liu [b], Andreas Jekle [b], Ruchika Jaisinghani [b], Suping Ren [b], Koen Vandyck [c], Dirk Jochmans [d], Pieter Leyssen [d], Johan Neyts [d], Lawrence M. Blatt [b], Leonid Beigelman [b], Julian A. Symons [b], Pierre Raboisson [c], Michael D. Scholle [a], Jerome Deval [b,*]

[a] SAMDI Tech, Inc, Chicago, USA
[b] Aligos Therapeutics, Inc, South San Francisco, USA
[c] Aligos Belgium BV, Leuven, Belgium
[d] Rega Institute, KU Leuven, Leuven, Belgium

ARTICLE INFO

Keywords:
COVID-19
Coronavirus
3CLpro
Protease inhibitor
SAMDI-MS
Mass spectrometry

ABSTRACT

Severe acute respiratory syndrome coronavirus 2 (SARS-CoV-2) is the cause of the COVID-19 pandemic that began in 2019. The coronavirus 3-chymotrypsin-like cysteine protease (3CLpro) controls replication and is therefore considered a major target for antiviral discovery. This study describes the evaluation of SARS-CoV-2 3CLpro inhibitors in a novel self-assembled monolayer desorption ionization mass spectrometry (SAMDI-MS) enzymatic assay. Compared with a traditional FRET readout, the label-free SAMDI-MS assay offers greater sensitivity and eliminates false positive inhibition from compound interference with the optical signal. The SAMDI-MS assay was optimized and validated with known inhibitors of coronavirus 3CLpro such as GC376 (IC_{50} = 0.060 μM), calpain inhibitors II and XII (IC_{50} ~20–25 μM). The FDA-approved drugs shikonin, disulfiram, and ebselen did not inhibit SARS-CoV-2 3CLpro activity in the SAMDI-MS assay under physiologically relevant reducing conditions. The three drugs did not directly inhibit human β-coronavirus OC-43 or SARS-CoV-2 *in vitro*, but instead induced cell death. In conclusion, the SAMDI-MS 3CLpro assay, combined with antiviral and cytotoxic assessment, provides a robust platform to evaluate antiviral agents directed against SARS-CoV-2.

1. Introduction

Severe acute respiratory syndrome coronavirus 2 (SARS-CoV-2) is the cause of the ongoing COVID-19 outbreak of respiratory illness first detected in Wuhan, China, in December 2019. In 2020, COVID-19 was declared a global pandemic, with worldwide confirmed cases exceeding 22 million infections and 750,000 deaths as of August 2020 (https://coronavirus.jhu.edu/map.html). The majority of infected individuals (>80%) are either completely asymptomatic or experience self-limiting symptoms similar to the common cold (Al-Tawfiq, 2020; Mizumoto et al., 2020). In its most severe form requiring hospitalization and intensive care, COVID-19 disease is characterized by high fever, pneumonia, and extra-pulmonary manifestations such as kidney failure, thrombosis (heart attack, pulmonary embolism, deep vein thrombosis, stroke), severe inflammation (cytokine storm), and central nervous system symptoms (encephalitis, seizures) (Harapan et al., 2020). According to the Centers for Disease Control and Prevention, risk factors include age ≥65 years and severe comorbidities such as heart, lung, and liver diseases, as well as immunocompromised state, diabetes, and obesity (https://www.cdc.gov/coronavirus/2019-ncov/need-extra-precautions/index.html).

The only antiviral drug currently approved under Emergency Use Authorization by the FDA for the treatment of COVID-19 hospitalized patients is remdesivir (200 mg intravenous loading dose, then 100 mg IV once daily) (Ison et al., 2020). In a clinical trial, remdesivir significantly reduced the time to recovery to 11 days versus 15 days with placebo control, with no significant effect on mortality (Beigel et al., 2020). Although many other antiviral agents have been or are being evaluated in clinic trials (e.g., favipiravir, baloxavir marboxil, HIV protease inhibitors, chloroquine and hydroxychloroquine, neuraminidase

* Corresponding author. Aligos Therapeutics, Inc, South San Francisco, United States.
E-mail address: jdeval@aligos.com (J. Deval).

https://doi.org/10.1016/j.antiviral.2020.104924
Received 3 July 2020; Received in revised form 21 August 2020; Accepted 22 August 2020
Available online 5 September 2020

inhibitors), none of these molecules were designed nor optimized specifically to treat coronavirus infection (https://www.goodrx.com/blog/coronavirus-treatments-on-the-way/). Therefore, and in the absence of any approved vaccines, there is a clear and urgent need to develop novel anti-coronavirus agents.

SARS-CoV-2 is an enveloped, positive-sense, single-stranded RNA virus that belongs to the β-coronavirus genus of the *Coronaviridae* family, which also includes SARS and MERS β-coronaviruses (Coronaviridae Study Group of the International Committee on Taxonomy of 2020). With a size of 26–32 kilobases, coronavirus genomes are considered the largest among RNA viruses. Viral RNA synthesis and processing are controlled by the nonstructural proteins (nsp) 7 to 16 after cleavage by the viral 3CL protease (3CLpro) of two large replicase polyproteins translated from the coronavirus genome. The main viral protease, 3CLpro, has a unique substrate preference for glutamine at the P1 site (Leu-Gln/(Ser,Ala,Gly)) (Fan et al., 2005). Along with 96% sequence identity with the SARS protein, the crystal structure of SARS-CoV-2 3CLPro revealed nearly identical protein structures between the two closely related viruses, with the conserved active site at the interface of domains I and II (residues 10–99 and 100–182, respectively) followed by domain III (residues 198–303) involved in regulating protein dimerization (Dai et al., 2020; Jin et al., 2020; Zhang et al., 2020). The 3CLpro enzyme controls replication and is therefore considered a major target for antiviral discovery. Discovery and functional characterization of protease inhibitors has historically relied on fluorescence resonance energy transfer (FRET) assays using a recombinant enzyme and short peptides labeled with a fluorescence emitter and quencher at each end of the sequence (Kuang et al., 2005; Liu et al., 2005; Zauner et al., 2011). Several small molecules have been recently reported to inhibit SARS-CoV-2 3CLpro in the FRET assay (Zhou et al., 2020). One of them, GC376, is a broad-spectrum peptidomimetic agent previously reported to inhibit noroviruses, picornaviruses, and coronaviruses (Kim et al., 2012; Takahashi et al., 2013; Kim et al., 2016; Pedersen et al., 2018). Shikonin, disulfiram, and ebselen are three FDA-approved drugs recently described to inhibit SARS-CoV-2 3CLpro enzymatic activity (Jin et al., 2020).

This study describes the evaluation of small molecule inhibitors with a novel SARS-CoV-2 3CLpro enzymatic assay. The approach combines self-assembled monolayers of alkanethiolates on gold with matrix-assisted laser desorption ionization time of flight (MALDI TOF) mass spectrometry. This methodology, termed SAMDI-MS, offers a label-free and high-throughput platform for measuring biochemical activity (Mrksich, 2008; Gurard-Levin et al., 2011; Patel et al., 2015). The assay was validated with 3CLpro inhibitors GC376, and calpain inhibitors II and XII. The SAMDI-MS assay also showed that the three FDA-approved drugs shikonin, disulfiram, and ebselen do not inhibit SARS-CoV-2 3CLpro activity under reducing conditions. These results are consistent with the general lack of anti-coronavirus effect and pronounced cytotoxicity for these three compounds. The relevance of these findings and their potential clinical implications are discussed.

2. Materials and methods

2.1. Proteins, peptides, and compounds

SARS-CoV-2 3CLpro was purchased from BPS Bioscience (San Diego, CA; Catalog 100707-1). Peptide substrates (Dabcyl-KTSAVLQSGFRKM-E (Edans)-NH_2 for FRET and Ac-TSAVLQSGFRKK(biotin)-NH_2 for SAMDI-MS) were sourced from Biopeptide (San Diego, CA) at >95% purity. Shikonin, disulfiram, and ebselen were purchased from Selleck Chemicals (Houston, TX), and their integrity in DMSO solution was verified by LC-MS (data not shown). GC376 was from Biosynth International (Oakbrook Terrace, IL). Calpain inhibitor II was from SigmaAldrich (St. Louis, MO). Calpain inhibitor XII was from Cayman Chemicals (Ann Arbor, MI).

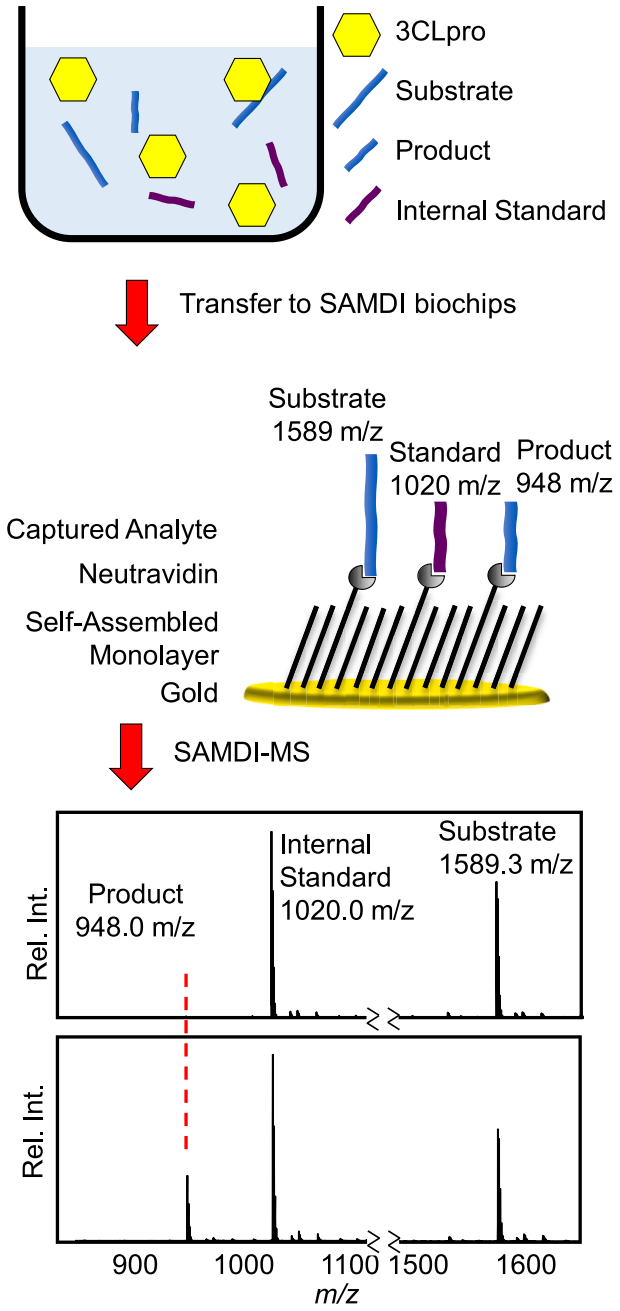

Scheme 1. Workflow of the SAMDI mass spectrometry assay of 3CLpro activity. (top) 3CLpro enzyme and substrate incubate in a homogenous reaction in a 384-well plate. (middle) The assay is quenched and transferred to high density biochip arrays featuring self-assembled monolayers of alkanethiolates on gold presenting Neutravidin to immobilize the biotinylated peptide substrate, product, and internal standard. (bottom) Representative SAMDI-MS spectra reveal peaks correfsponding to substrate, product, and internal standard.

2.2. 3CLpro mass spectrometry assay

Protease assays were performed in 6 μL volume in 384-well low volume polypropylene microtiter plates (Greiner Bio-One, Kremsmünster, Austria; Catalog 784201) at ambient temperature. The optimized assay buffer was 20 mM Hepes pH 8.0, 10 mM NaCl, 1 mM EDTA, 0.005% bovine skin gelatin (BSG), 0.002% Tween-20, 1 mM

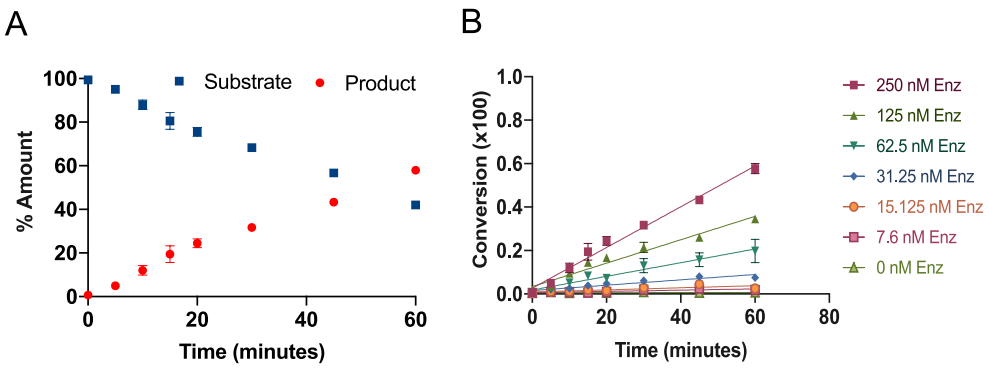

Fig. 1. SAMDI-MS to analyze 3CLpro activity (A) The loss of substrate and growth of product over time is calculated using SAMDI-MS. (B) The product of 3CLpro measured by SAMDI-MS increases with increasing enzyme (Enz) concentrations. All measurements from triplicate data. Product analyzed using a linear fit with $R^2 > 0.98$.

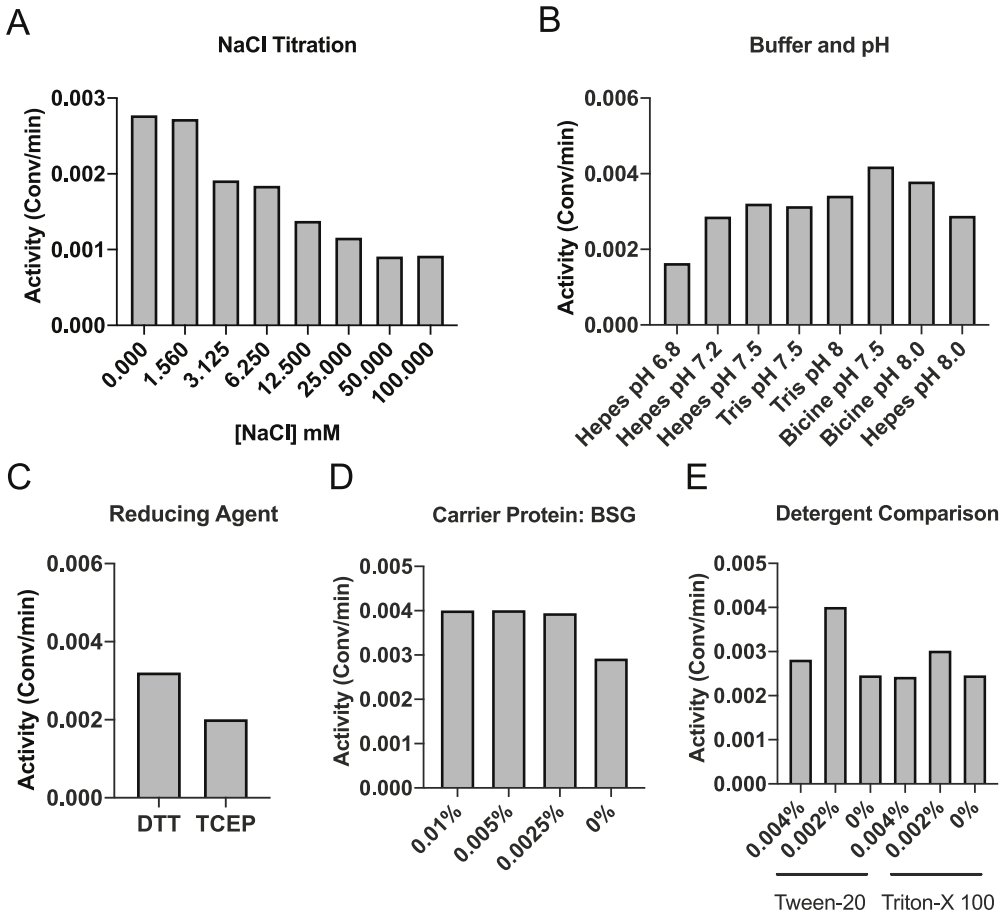

Fig. 2. Buffer optimization of SAMDI-MS assay. The initial velocity calculated from triplicate data utilizing the linear range of 3CLpro activity over a range of distinct conditions: (A) NaCl concentration from 0 to 100 nM, (B) buffer (Hepes, Tris, and Bicine) and pH (6.8–8.0), (C) reducing agent (DTT and TCEP at 1 mM), (D) bovine skin gelatin (BSG)—a carrier protein—concentration), and (E) detergent Tween-20 and Triton-X 100.

dithiothreitol (DTT). For compound screening, 3CLpro (final concentration 125 nM) was added using a Multidrop Combi (Thermo Scientific; Waltham, MA) and preincubated for 30 min with small molecules. Reactions were initiated by the addition of the peptide substrate (final concentration 10 μM). Reactions were incubated for 90 min and quenched by the addition of 0.5% formic acid (final) with subsequent neutralization using 1% sodium bicarbonate (final). An internal standard peptide was added (Ac-SAYRKK(biotin)-NH_2) in 20 mM Hepes pH 8.0 to a final concentration of 1 μM for quantitation of the protease product. For SAMDI-MS analysis, 2 μL of each reaction mixture was transferred using a 384-channel automated liquid handler to SAMDI biochip arrays functionalized with a neutravidin-presenting self-assembled monolayer. The preparation of SAMDI biochip arrays has been previously described (Gurard-Levin et al., 2011). The SAMDI arrays were incubated for 1 h in a humidified chamber to allow the specific immobilization of the biotinylated peptide substrate, cleaved product, and internal standard. The samples were purified by washing the SAMDI arrays with deionized ultrafiltered water (50 μL/spot) and dried with

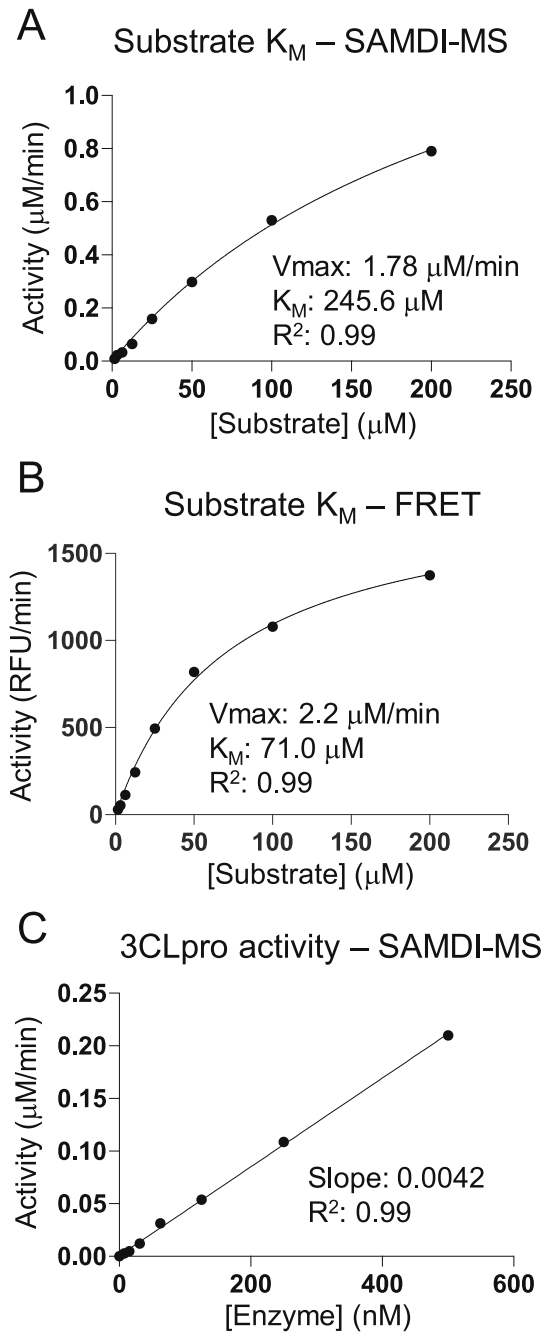

Fig. 3. K_M and V_{max} values determined using SAMDI-MS and FRET assay. (A) K_M values were determined for the (A) SAMDI and (B) FRET assay formats (corrected for inner filter effect). (C) Velocity of 3CLpro is linear over a range of concentrations in the SAMDI-MS assay using 10 μM substrate. All measurements from triplicate data.

compressed air. A matrix comprising alpha-cyano cinnamic acid in 80% acetonitrile:20% aqueous ammonium citrate (10 mg/mL final) was applied in an automated format by dispensing 50 nL to each spot in the array. SAMDI-MS was performed using reflector-positive mode on an AB Sciex TOF-TOF 5800 System (AB Sciex, Framingham, MA) with 400 shots/spot analyzed in a random raster sampling. For data analysis, area under the curves (AUCs) for the product peak and internal standard were calculated using the TOF/TOF Series Explorer (AB Sciex) and the amount of product formed was calculated using the equation ($AUC_{product}/AUC_{internal\ standard}$). The amount of product generated was calculated using the ratio of product area under the curve (AUC) divided by the AUC of the internal standard. Negative controls were pre-quenched with 0.5% formic acid final. Assay robustness was determined by Z-Factor, calculated using equation 1 – (3 (σpos+σneg)/(μpos-μneg)) where σ is the standard deviation and μ is the average conversion of the positive and negative control wells.

2.3. FRET-based assay

The FRET-based assay was performed similarly to the SAMDI-MS assay. Assays were performed in 6 μL volume in 384-well shallow ProxiPlate-Plus microtiter plates (PerkinElmer; Waltham, MA) at ambient temperature in the optimized assay buffer described in Section 2.2. Reactions were initiated by the addition of a FRET-compatible peptide substrate Dabcyl-KTSAVLQSGFRKM-E (Edans)-NH_2. Fluorescence was measured at 90 min using a 340/460 excitation/emission filter module on a Pherastar FS plate reader (BMG Labtech; Ortenberg, Germany). To account for the inner filter effect, free EDANS (5- [(2-aminoethyl)amino]naphthalene-1-sulfonic acid) (Anaspec; Fremont, CA) was titrated in the presence and absence of the FRET substrate at equimolar ratios and the fluorescence was measured. The fluorescence in the presence of substrate was divided by the fluorescence for EDANS alone to give a correction value for each concentration. The initial velocity observed was then divided by the corresponding correction value to generate the Michaelis–Menten kinetics constant (K_M).

2.4. OC43–CoV coronavirus assay in MRC-5 and HeLa cells

The human beta-coronavirus OC43–CoV was purchased from ATCC (Manassas, VA) and propagated using HCT-8 human colorectal epithelial cells (ATCC). HeLa human cervical epithelial cells (ATCC) and MRC-5 human lung fibroblast cells (ATCC) were used as susceptible host cell lines and were cultured using EMEM media supplemented with 10% fetal bovine serum (FBS), 1% (v/v) penicillin/streptomycin (P/S), 1% (v/v) Hepes, and 1% (v/v) Cellgro Glutagro™ supplement (all Corning; Manassas, VA) at 37 °C. For the OC43–CoV antiviral assay, 1.5×10^4 HeLa cells per well or 1.0×10^4 MRC-5 cells per well were plated in 100 μL complete media in white 96-well plates with clear bottoms at 37 °C for up to 24 h to facilitate attachment and allow cells to recover from seeding stress. The next day, the cell culture medium was removed. Serially diluted compounds in 100 μL assay media (EMEM, 2% FBS, 1% P/S, 1% Cellgro Glutagro supplement, 1% Hepes) were added to the cells and incubated for 4 h at 37 °C in a humidified 5% CO_2 incubator. An aliquot of 100 μL of OC43–CoV virus stock was diluted to a concentration known to produce optimal cytopathic effect, inducing 80%–90% reduction in cell viability. Each 96-well plate was incubated for 5 days (for MRC-5 cells) or 6 days (for HeLa cells) at 33 °C; each plate included uninfected control wells and virus-infected wells that were not treated with compound. Cytotoxicity plates without the addition of OC43–CoV virus were carried out in parallel. At the end of the incubation period, 100 μL cell culture supernatant was replaced with 100 μL CellTiter-Glo® reagent (Promega; Madison, WI) and incubated for at least 10 min at room temperature prior to measuring luminescence. Luminescence was measured on a PerkinElmer Envision plate reader. Antiviral % inhibition was calculated using GraphPad (San Diego, CA) Prism software version 8.3.1, as follows:[(Compound treated cells infected sample) – (no compound infected control)]/[(Uninfected control) – (no compound infected control)]*100. The antiviral dose-response plot was generated as a sigmoidal fit, log (inhibitor) vs response-variable slope (four parameters) model and the compound concentration corresponding to a 50% inhibition of the viral cytopathic effect (EC_{50}) was calculated.

2.5. SARS-CoV-2 antiviral and toxicity assays

The SARS-CoV-2 antiviral assay is derived from the previously established SARS-CoV assay (Ivens, Van den Eynde et al., 2005). The test compounds were serially diluted in cell culture medium consisting in

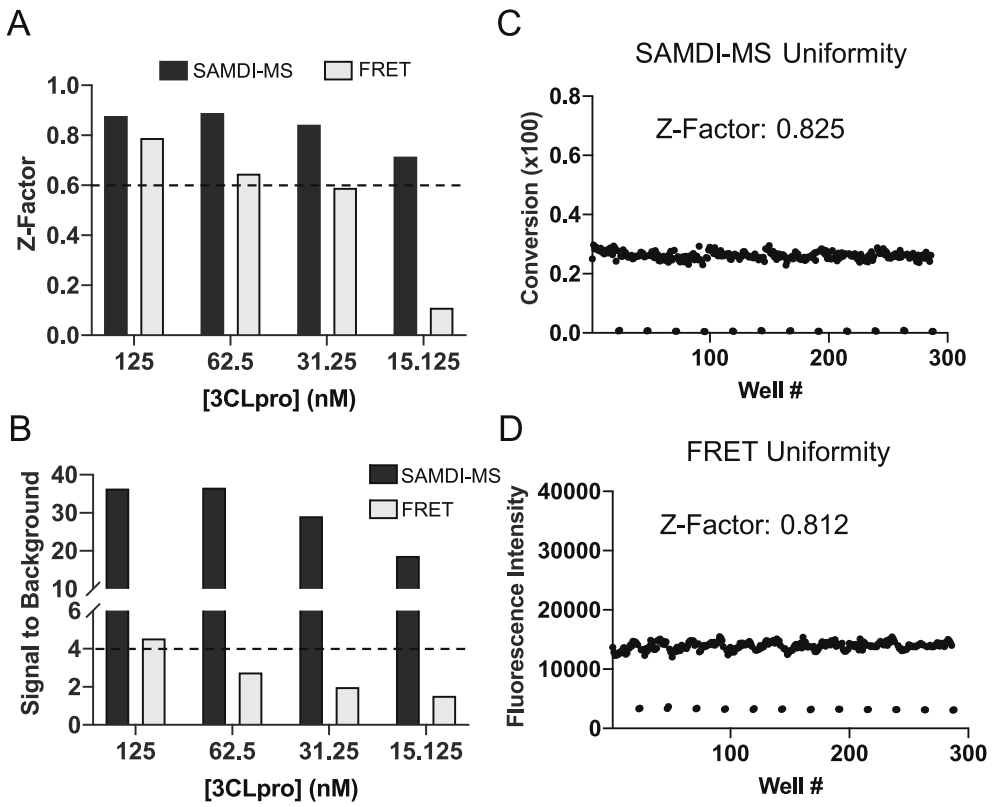

Fig. 4. Robustness –determined using Z-factor—(A) and signal to background ratios (B) for SAMDI-MS and FRET assays under different enzyme concentrations. The dotted line indicates an assay robustness cutoff of 0.6 for Z-factor, and 4-fold for signal to background. (C) Full plate uniformity data using optimized conditions and 6 μL reaction volumes for SAMDI-MS (C) and FRET (D) assays. Low controls for FRET lacked enzyme while low controls for the SAMDI-MS assay were pre-quenched with 0.5% formic acid (final).

DMEM (Gibco cat no 41965-039) supplemented with 2% v/v heat-inactivated FCS and sodium bicarbonate (Gibco 25080-060). Diluted compounds were then mixed with SARS-CoV-2 (SARS2_Belgium_20200414) at 20 TCID50/well and VeroE6-EGFP cells corresponding to a final density of 25,000 cells/well in 96-well blackview plates (Greiner Bio-One, Vilvoorde, Belgium; Catalog 655090). The plates were incubated in a humidified incubator at 37 °C and 5% CO_2. After 4 days, the wells were examined for EGFP expression using an argon laser-scanning microscope. The microscope settings were excitation at 488 nm and emission at 510 nm and the fluorescence images of the wells were converted into signal values. The results were expressed as EC_{50} values defined as the concentration of compound achieving 50% inhibition of the virus-reduced EGFP signals as compared to the untreated virus-infected control cells. Toxicity of compounds in the absence of virus was evaluated in the standard MTS-assay (Jochmans et al., 2012).

3. Results

3.1. Development of a mass spectrometry assay of SARS-CoV-2 3CLpro activity

To develop a self-assembled monolayer desorption ionization mass spectrometry (SAMDI-MS) based enzymatic assay for 3CLpro activity, we designed a peptide substrate featuring the canonical glutamine cleavage site positioned centrally within the sequence (Ac-TSAVLQSGFRKK(biotin)-NH2) and a lysine biotinylated at the epsilon amino group (Fan et al., 2005). Following a homogenous reaction in a 384-well plate, the reactions are transferred to SAMDI biochips where the biotinylated side chain allows for the specific immobilization onto neutravidin-presenting self-assembled monolayers. Upon 3CLpro activity, the resulting product (SGFRKK(biotin)-NH2 is distinctly resolved in the SAMDI-MS spectrum (Scheme 1, Supplementary Figure 1A). To quantitatively assess protease product yield in an MS assay, it is important to consider differences in ionization efficiency between the substrate and product. To test ionization efficiency, eight distinct ratios of product and substrate were prepared and analyzed by SAMDI-MS. The spectra revealed the substrate peak at 1589.3 m/z and the product at 948.0 m/z. The amount of product observed is calculated using the equation $AUC_{prod}/(AUC_{sub} + AUC_{prod})$ and results in a non-linear relationship indicating that the product exhibits higher ionization efficiency than the substrate (Supplementary Fig. 1B). To facilitate quantitative analysis, an internal standard peptide was designed that differs from the product (SAYRKK(biotin)-NH2) by mass but features similar properties and is therefore likely to exhibit similar ionization efficiency. Ionization efficiencies of the product and standard were then compared by preparing eight distinct ratios of product and standard and the amount of product calculated directly correlates with the prepared ratios (Supplementary Fig. 1C). Notably, the internal standard was added post-reaction to avoid altering enzyme activity. The peptide substrate was then incubated with 3CLpro and the reaction monitored by SAMDI-MS. The substrate peak decreased over time and the product peak increased (Fig. 1A, Supplementary Table 1 3CLpro activity was further characterized over a range of concentrations and the product formed measured by SAMDI-MS. Product formation increased as enzyme concentration increased over the range of 7.6–250 nM (Fig. 1B). Taken together, these data support the use of the peptide substrate in the development of the first reported label-free SARS-CoV-2 3CLpro activity assay.

3.2. Optimization of assay conditions and determination of kinetic constants

Assay development is a critical process in drug discovery to optimize assay conditions suitable for characterizing candidate modulators. SAMDI-MS assay development of 3CLpro was performed in parallel with the traditional FRET-based readout using the FRET-compatible substrate dabcyl-KTSAVLQSGFRKM-E (Edans)-NH_2. The impact of salt concentration was tested by titrating NaCl from 0 to 100 mM and the results showed that while 3CLpro fairly well tolerated salt concentrations up to

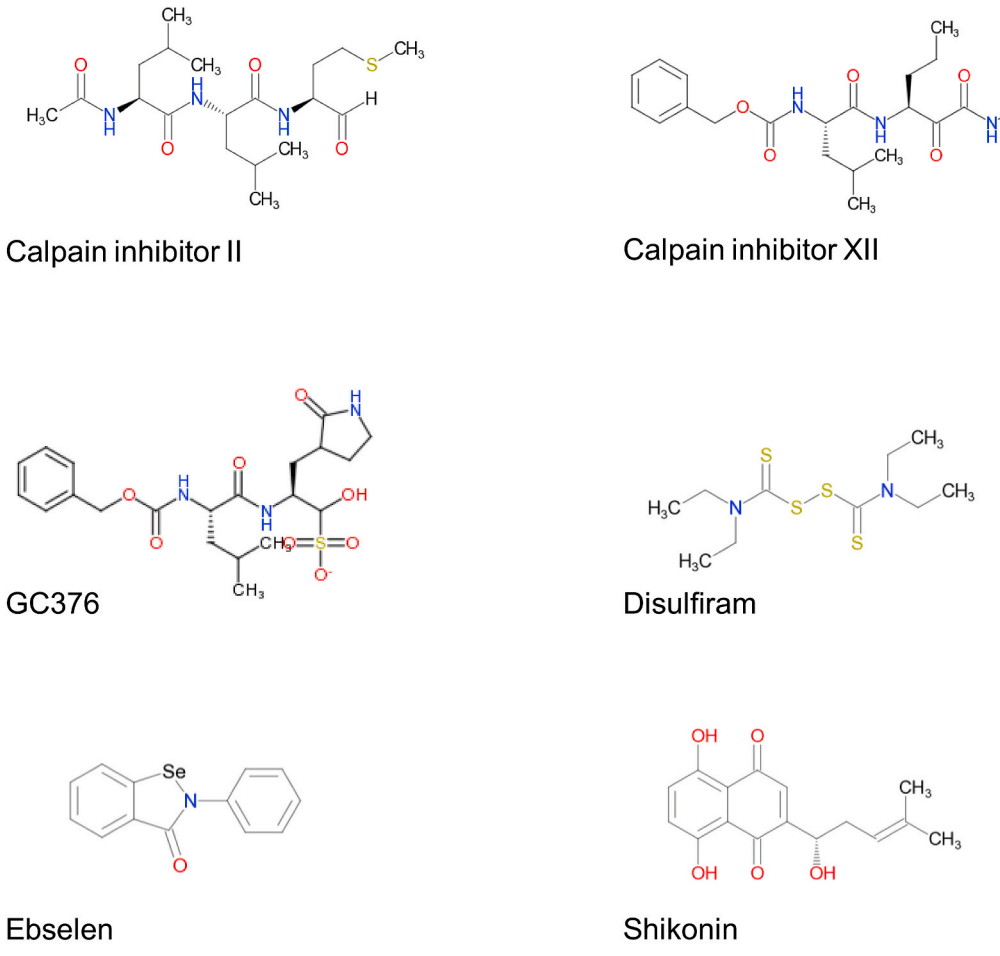

Fig. 5. Structures of six reported 3CLpro inhibitors.

Table 1
Summary of inhibition of SARS-CoV-2 3CLpro in FRET and SAMDI-MS assay.

Test Article	IC_{50} (μM)	
	FRET Assay	SAMDI-MS Assay
GC376	0.052 ± 0.007	0.060 ± 0.019
Calpain Inhibitor II	8.98 ± 2.0	24.76 ± 7.5
Calpain Inhibitor XII	6.48 ± 3.4	21.0 ± 8.5
Ebselen	>100	>100
Disulfiram	>100	>100
Shikonin	15.0 ± 3.0	>100

100 mM, the reaction rate was fastest in the absence of salt (Fig. 2A, FRET-based data in Supplementary Fig. 2A). Titrating KCl generated similar results (data not shown). The 10 mM NaCl condition was used to ensure sufficient activity while maintaining some ionic strength in the reaction as the impact of buffer and pH was evaluated. The data highlight that 3CLpro retained activity between pH 7–8 and in the presence of a variety of buffer salts (Fig. 2B, FRET-based data in Supplementary Fig. 2B), which corroborated previous reports using label-based assay methodologies (Grum-Tokars et al., 2008). Next, the effect of reducing agents was examined using DTT and tris(2-carboxyethyl)phosphine) (TCEP), as well as the presence of detergents Tween-20 and Triton-X 100, and the carrier protein bovine skin gelatin (BSG) (Fig. 2C-E, FRET-based data in Supplementary Fig. 2C–2E). The data for both assay formats converge on an optimal buffer comprising 20 mM Hepes pH 8.0, 10 mM NaCl, 1 mM EDTA (to remove trace metals that could be present in small molecule preparations), 0.005% BSG, 0.002% Tween, and 1 mM DTT.

With the optimized buffer, the K_M and maximum velocity (V_{max}) of the peptide substrate was measured using SAMDI-MS and FRET. The peptide concentration was titrated between 1.5 and 200 μM and the product monitored over time. Plotting the initial velocity of the linear portion versus the substrate concentration revealed distinct curves for the two assay formats. The SAMDI-MS assay generated a traditional Michaelis-Menten curve with an apparent K_M of 245 μM and a V_{max} of 1.78 μM/min (Fig. 3A). In the FRET assay, protease activity increased with substrate concentration until 50 μM, after which the signal started to decrease due to the inner filter effect (Supplementary Figure 3A). The inner filter effect impacts the fluorescence intensity at substrate concentrations >20 μM due to intermolecular quenching from neighboring uncleaved peptides (Palmier and Van Doren, 2007). Correcting for this effect (Supplementary Figure 3B) generated a traditional Michaelis-Menten curve with an apparent K_M of 71 μM and a V_{max} of 1869 relative fluorescence units (RFU)/min, or 2.2 μM/min (Fig. 3B, Supplementary Figure 3C), in line with the MS assay. For both assay formats, 10 μM peptide (a concentration below K_M) was selected to allow for the discovery and characterization of substrate-competitive inhibitors while also ensuring suitable conversion of substrate to product for a robust assay. Using these conditions, conversion was measured by SAMDI-MS at various enzyme concentrations in the presence of 1% DMSO to mimic the presence of compounds and revealed linear enzyme activity up to 500 nM enzyme (Fig. 3C).

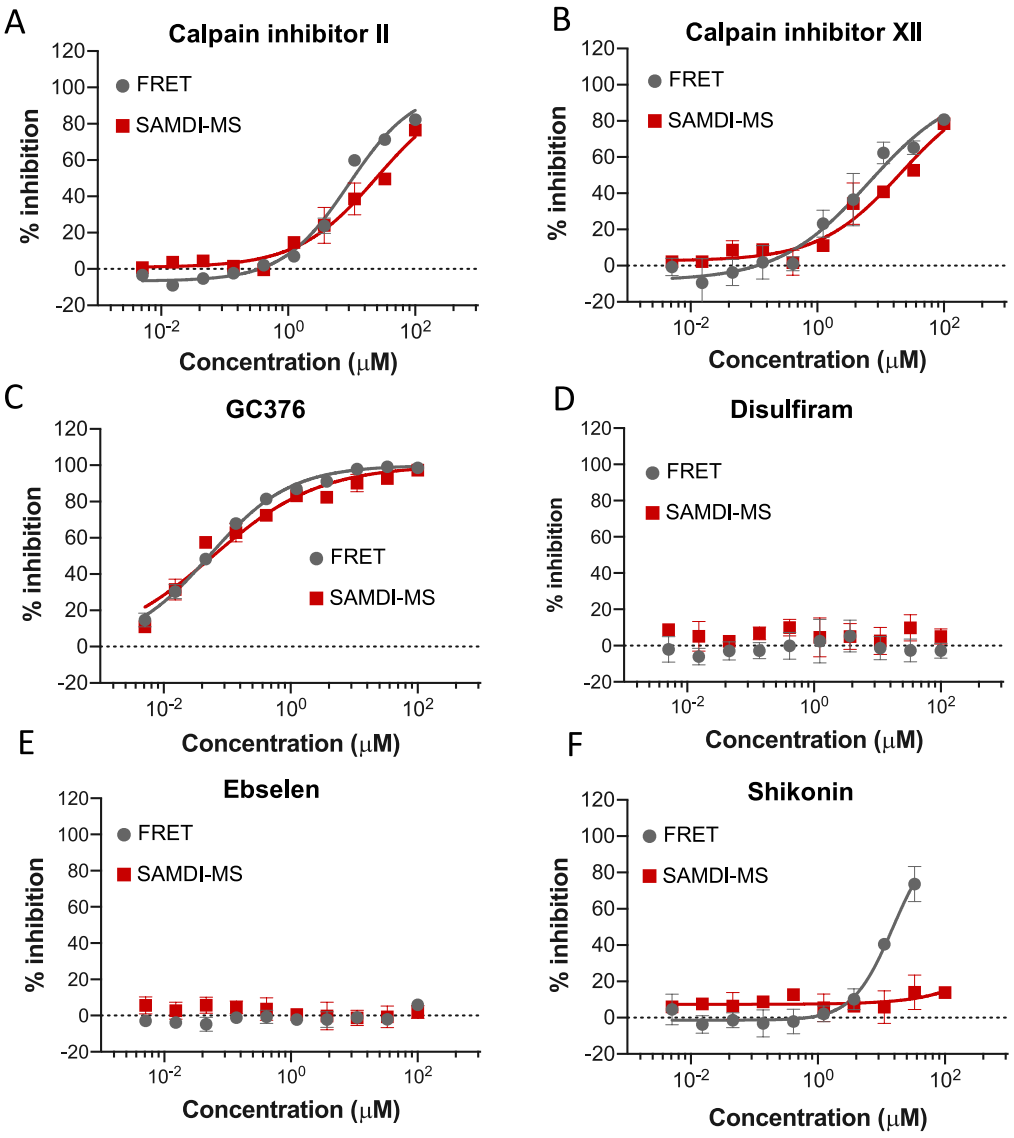

Fig. 6. IC_{50} measurements of six reported 3CLpro inhibitors were calculated in the SAMDI-MS (red) and FRET (grey) assay formats. Experiments were performed in duplicate and error bars represent standard deviation. IC_{50} values reported in Table 1.

3.3. Assay performance and validation with positive controls of 3CLPro inhibition

Given that robustness of screening assays is critical to quantitatively measure compound potency, the robustness of the SAMDI-MS and FRET assay formats were assessed in 6 μL volumes in 384-plate format using the optimized conditions between 15 nM and 125 nM 3CLpro. The presence of positive and negative controls permitted calculation of a Z-factor (a measure of robustness), which considers the mean and standard deviation for positive and negative controls. The data show that the robustness of the SAMDI-MS assay is maintained even at 15 nM enzyme (Z-factor >0.7), whereas at this enzyme concentration the FRET assay produces a Z-factor of 0.1 well below the acceptable cutoff of 0.5–0.6 (Fig. 4A). Moreover, comparing the signal to background (S/B) across the two assay formats highlights a superior S/B using SAMDI-MS at all enzyme concentrations tested. For example, at 15 nM enzyme the S/B by SAMDI-MS is ~20x compared to 1.5x for FRET. Even at 125 nM 3CLpro, the S/B in the FRET assay is approximately 4x, compared to 36x in the SAMDI-MS assay (Fig. 4B). With the main goal focused on comparing inhibitors in two assay formats, 125 nM 3CLpro was selected in order to generate robust results (Z-factor > 0.8) with each assay methodology to maintain comparable conditions of enzyme concentration (Fig. 4C and D). Next, we evaluated reported 3CLpro inhibitors (Fig. 5) in each assay format. The calpain inhibitors II and XII resulted in largely similar IC_{50} values in the FRET (8.98 ± 2.0 and 6.48 ± 3.4 μM, respectively) and SAMDI-MS (24.8 ± 7.5 and 21.0 ± 8.5 μM, respectively) assays (Table 1) (Fig. 6A and B). The known inhibitor GC376 had a measured IC_{50} value of 0.052 ± 0.007 μM in the FRET assay and 0.060 ± 0.019 μM in the SAMDI-MS assay (Fig. 6C). The IC_{50} values of ebselen and disulfiram were >100 μM both in the FRET and SAMDI-MS assays (Fig. 6D and E). Shikonin exhibited an IC_{50} value of 15.0 ± 3.0 μM in the FRET assay but failed to inhibit 3CLpro in the SAMDI-MS assay (Fig. 6F). Given the deep red color of this compound at high concentrations and its reported fluorescence in the visible spectrum, it is likely that the color interfered with the fluorescence signal in the FRET assay (Wiench et al., 2012). To address that hypothesis, a FRET assay was initiated using the optimized conditions in the absence of compound and the plate analyzed at 90 min. Immediately upon reading the plate, a titration of shikonin was added to the same wells and the plate was reanalyzed. The wells with high concentrations of shikonin exhibited a decrease in fluorescence, supportingthe hypothesis that shikonin quenches the FRET signal, and therefore represents a false positive due to optical interference

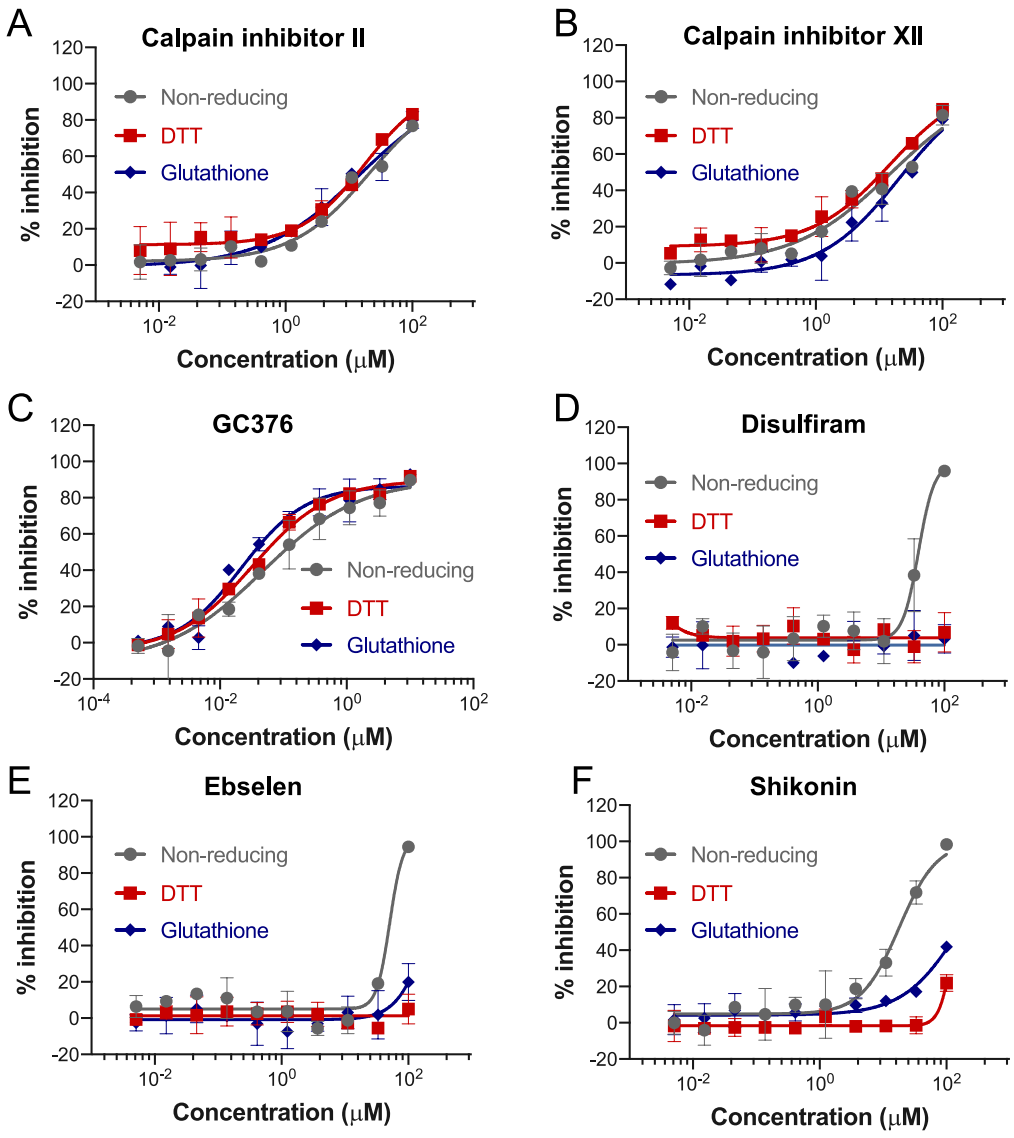

Fig. 7. IC_{50} measurements of 6 reported 3CLpro inhibitors measured by SAMDI-MS in the absence of reducing agent (grey), in the presence of 1 mM DTT (red), and in the presence of 1 mM glutathione (blue). Experiments were performed in duplicate and error bars represent standard deviation.

(Supplementary Figure 4).

3.4. Effect of reducing conditions on SARS-CoV-2 3CLpro inhibition

3CLpro is a cysteine protease and inhibition may be dependent on oxidation state. To understand the contribution of oxidative state to compound inhibition in the biochemical assay, the same inhibition experiments were conducted in the SAMDI-MS assay under three different conditions: no reducing agent, weak (glutathione (GSH)) and strong (DTT) reducing conditions. The reducing conditions had no effect on the inhibition potency of the two calpain inhibitors and GC376 (Fig. 7A, B, and C). However, inhibition potencies of ebselen, disulfiram, and shikonin were impacted by the reducing condition of the assay. Ebselen and disulfiram only inhibited SARS-CoV-2 3CLpro at concentrations >30 μM and in the absence of reducing agent (Fig. 7D and E). Likewise, shikonin inhibited the protease mainly in the absence of reducing agent, with marked loss of inhibition in the presence of DTT or GSH (Fig. 7F).

3.5. Antiviral effect against human beta-coronavirus OC43–CoV and SARS-CoV-2 in cell culture

The same six small molecules were tested for inhibition of OC43, another human beta-coronavirus used as a Biosafety Level 2 surrogate for SARS-CoV-2. Because OC43–CoV is cytopathic to HeLa cells after 6 days post-infection, rescue of cells with compound from virus-induced cytopathic effect was used as an indirect measurement of virus inhibition and reported as EC_{50}. Compound-induced cytotoxic effect (CC_{50}) was determined in the absence of viral infection for the same incubation period, in parallel with EC_{50}. In the HeLa cytopathic effect assay, remdesivir, the inhibition control of virus replication, had EC_{50} and CC_{50} values of 0.114 ± 0.009 and >1 μM, respectively (Table 2). GC376 was the most active protease inhibitor tested with sub-micromolar EC_{50} values. The calpain inhibitors II and XII had antiviral activity with EC_{50} values of 20.7 and 15.2 μM, respectively, while ebselen, disulfiram and shikonin were inactive and cytotoxic. To understand the contribution of the cell line to antiviral potency and cytotoxicity, similar experiments were conducted in the MRC-5 cell line derived from human lung fibroblasts. In the MRC-5 assay, EC_{50} and CC_{50} values for all six compounds were in good agreement with those obtained with HeLa cells (Table 2,

Table 2
Summary of antiviral effect against human OC43–CoV and SARS-CoV-2 in cell culture.

Test Article	OC-43 Hela Cells		OC-43 MRC-5 Cells		SARS-CoV-2 VeroE6 Cells	
	EC_{50} (μM)	CC_{50} (μM)	EC_{50} (μM)	CC_{50} (μM)	EC_{50} (μM)	CC_{50} (μM)
Remdesivir	0.114 ± 0.009	>1	0.21	≥50	n.d.	n.d.
GS-441524	n.d.	n.d.	n.d.	n.d.	<0.8	55 ± 18
GC376	0.42 ± 0.033	>10	0.83	>50	10 ± 4.2	>100
Calpain Inhibitor II	20.7 ± 3.3	>100	20.95	>100	27 ± 1.4	>100
Calpain Inhibitor XII	15.2 ± 2.4	60.3 ± 8.3	6.93	>50	1.3 ± 0.57	27 ± 0.0
Ebselen	>100	15.9 ± 2.4	>100	8.23	>100	37.5 ± 9.2
Disulfiram	>100	75	>100	8.35	>100	13.5 ± 0.70
Shikonin	>100	1.4 ± 0.001	>100	0.32	>100	1.55 ± 0.07

Footnote: n.d. = non determined.

Supplementary Figure 5). Ebselen, disulfiram, and shikonin were also cytotoxic in MRC-5 cells with CC_{50} values of 8.23, 8.35, and 0.32 μM, respectively.

Finally, the antiviral potency of these compounds was evaluated against SARS-CoV-2. The SARS-CoV-2 antiviral assay was adapted from the previously established SARS-CoV assay, using Vero cells engineered to constitutively express an enhanced green fluorescent protein (Ivens, Van den Eynde et al., 2005). In this cytopathic effect assay, GS-441524, the parent molecule of remdesivir, was used as positive control for EC_{50} determination (Table 2). Although individual SARS-CoV-2 EC_{50} values were somewhat different from those obtained with OC43–CoV, there was a general trend of good separation between antiviral potency and cytotoxicity for GC376 and calpain inhibitor II and XII. As previously observed with OC43–CoV, ebselen, disulfiram, and shikonin did not inhibit SARS-CoV-2 replication, but instead were toxic to Vero cells. Shikonin was the most toxic compound with a CC_{50} value of 1.55 ± 0.07 μM. In conclusion, compounds exhibiting inhibition in the label-free SAMDI-MS assay proved to be the most effective against OC43–CoV and SARS-CoV-2 in cells.

4. Discussion

This study reports the first label-free and high-throughput assay to measure coronavirus 3CLpro activity and opens avenues for improved drug discovery efforts to find small molecule inhibitors to treat COVID-19. The SAMDI-MS technology has been reported to characterize dozens of biochemical activities including post-translational modifying enzymes (Gurard-Levin et al., 2011; Swalm et al., 2014; Patel et al., 2015; Wigle et al., 2015; Szymczak et al., 2018; O'Kane et al., 2019), RNA-modifying proteins (Buker et al., 2020), and proteases (Min et al., 2004) and can be applied to virtually any enzymatic activity. While the FRET-based assay format is convenient and can easily be adopted by standard biochemistry labs, this study demonstrates that SAMDI-MS offers distinct advantages over label-dependent FRET that were critical in developing the SARS-CoV-2 3CLpro assay (Fig. 2, Supplementary Figure 2). First, SAMDI-MS eliminates the fluorescent label, which prevents spurious interactions between fluorescent labels and the enzyme that could alter enzyme activity and specificity. In one particular example, activation of the SIRT1 deacetylase by the small molecule resveratrol was dependent on the fluorescent substrate (Kaeberlein et al., 2005). Second, the Dabsyl-Edans emitter-quencher combination is susceptible to the inner filter effect that results from intermolecular quenching (Fig. 3), which limits the substrate concentrations that can be reliably tested and complicates K_M determination (Liu et al., 1999; Blanchard et al., 2004; Grum-Tokars et al., 2008). While reported correction factors are appropriate when dealing with substrate alone (Liu et al., 1999), it is important to consider the impact of small molecules that may exhibit similar behavior when tested at high concentrations. Finally, while salts and detergents can induce ion suppression in conventional MS techniques, the SAMDI-MS technology is amenable to a large range of buffer components due to the specific immobilization of the analyte, while other components are washed away. This capability enables the development of assay conditions that are optimal for the target, rather than for the detection methodology. While this study required the use of a biotin group to specifically immobilize the peptide substrate, product, and internal standard, alternative approaches are available for analyte immobilization in cases where a biotin may impact enzyme activity (Gurard-Levin et al., 2011).

The data also demonstrate a significantly improved sensitivity, robustness, and signal to background ratio in the SAMDI-MS assay relative to the traditional FRET approach. (Fig. 4). Part of the SAMDI-MS assay validation consisted in evaluating the potency of a representative set of reported 3CLpro active site inhibitors consisting of GC376, calpain inhibitors II and XII shikonin, disulfiram, and ebselen (Kim et al., 2012; Jin et al., 2020; Ma et al., 2020). The IC_{50} values of GC376 were generally in good agreement with prior reports, while in our study calpain inhibitors II and XII were less potent (Ma et al., 2020). The data also highlight that while most compounds exhibit similar IC_{50} values between the two enzymatic assay platforms, the SAMDI-MS assay is not prone to false positive and false negative results due to fluorescence quenching or autofluorescence of small molecules present in screening collections. In one example, the data illustrate that the reported 3CLpro inhibitor shikonin represents a false positive due to the nature of the fluorescence assay (Fig. 6 and Supplementary Figure 4). Characterizing small molecules with SAMDI-MS ensures that only the most promising candidate compound progress toward lead optimization, saving time and resources with benefits shared by researchers and ultimately, the patients.

Shikonin, disulfiram, and ebselen were recently described to inhibit SARS-CoV-2 3CLpro in a FRET enzymatic assay (Jin et al., 2020). In our study, neither one of these molecules inhibited 3CLpro in the SAMDI-MS or FRET assays. Since Jin et al. conducted their enzymatic assays in the absence of reducing agents, our surprising results led us to evaluate the impact of the oxidative state of the biochemical assay on inhibition potency. The reducing conditions had no effect on the inhibition potency of the two calpain inhibitors and GC376 (Fig. 7). However, the inhibition potencies of ebselen, disulfiram, and shikonin were negatively impacted by the presence of reducing agents. Although DTT is a strong reducing agent, GSH is weaker and also considered the primary intracellular physiological reducing agent in human cells (Lee et al., 2012). Both ebselen and disulfiram are described to covalently modify cysteine residues and similar impact of DTT on the *in vitro* activity of ebselen and disulfiram has been described for glucosyltransferase domain inhibition (Beilhartz et al., 2016) and liver mitochondrial aldehyde dehydrogenase (Shen et al., 2000) respectively. Shikonin is described to react with thiols (Gao et al., 2002). Shikonin is also reported to act on caspase-1, likely by reacting with the cysteine moiety (Zorman et al., 2016), and its 1, 4-naphtoquinone scaffold has been described as a cysteine protease inhibitor (Valente et al., 2007). Therefore, it is unclear if the observed inactivation effect of DTT and GSH is due to direct reactivity with shikonin or via another mechanism. A similar protective effect has been noted for the action of DTT on inactivation of GAPDH by 1,

4-benzoquinone (Rodriguez et al., 2005). Therefore, the impact of the lack of inhibitory effect of these FDA-approved drugs on SARS-CoV-2 3CLpro in the presence of physiologically relevant levels of GSH will have to be further investigated with additional antiviral testing. In the case of GC376 and calpain inhibitors, our cell-based data with human β-coronavirus OC43–CoV and SARS-CoV-2 indicated a significant window between antiviral potency and cytotoxicity, consistent with direct inhibition of 3CLpro (Table 2). However, shikonin, disulfiram, and ebselen did not show any signs of antiviral activity on human β-coronavirus OC43–CoV or SARS-CoV-2 (Table 2). Instead, these three drugs were toxic in the three evaluated cell lines. Our hypothesis, supported by the data presented here, is that the reported antiviral effect of ebselen against SARS-CoV-2 using qRT-PCR is an indirect consequence of cell death (Jin et al., 2020). Taken together, our biochemical and cell-based results converge to indicate a lack of direct antiviral activity of these three drugs, bringing further questions on their use as potential coronavirus treatment.

In conclusion, the SAMDI-MS technology offers an alternative method for high-throughput screening of 3CLpro and related virus proteases with advantages in sensitivity, selectively, and robustness. Furthermore, our data indicate that protease inhibitors that maintain a biochemical potency against SARS-CoV-2 3CLpro in the presence of physiologically relevant reducing agents are more likely to inhibit virus replication in cells, and therefore present higher potential for efficacy in humans.

5. Funding

Aligos Therapeutics provided funding for this study but did not have any additional role in the study design, data collection and analysis, decision to publish, or preparation of the manuscript.

Acknowledgements

We thank Peggy Korn for her careful editorial review of the manuscript, and Caroline Williams for LC-MS analysis.

Appendix A. Supplementary data

Supplementary data to this article can be found online at https://doi.org/10.1016/j.antiviral.2020.104924.

References

Al Tawfiq, J.A., 2020. Asymptomatic coronavirus infection: MERS-CoV and SARS-CoV-2 (COVID-19). Trav. Med. Infect. Dis. 101608.

Beigel, J.H., Tomashek, K.M., Dodd, L.E., Mehta, A.K., Zingman, B.S., Kalil, A.C., Hohmann, E., Chu, H.Y., Luetkemeyer, A., Kline, S., Lopez de Castilla, D., Finberg, R. W., Dierberg, K., Tapson, V., Hsieh, L., Patterson, T.F., Paredes, R., Sweeney, D.A., Short, W.R., Touloumi, G., Lye, D.C., Ohmagari, N., Oh, M.D., Ruiz-Palacios, G.M., Benfield, T., Fatkenheuer, G., Kortepeter, M.G., Atmar, R.L., Creech, C.B., Lundgren, J., Babiker, A.G., Pett, S., Neaton, J.D., Burgess, T.H., Bonnett, T., Green, M., Makowski, M., Osinusi, A., Nayak, S., Lane, H.C., Members, A.-S.G., 2020. Remdesivir for the treatment of Covid-19 - preliminary report. N. Engl. J. Med. https://doi.org/10.1056/NEJMoa2007764.

Beilhartz, G.L., Tam, J., Zhang, Z., Melnyk, R.A., 2016. Comment on "A small-molecule antivirulence agent for treating Clostridium difficile infection. Sci. Transl. Med. 8 (370), 370tc372.

Blanchard, J.E., Elowe, N.H., Huitema, C., Fortin, P.D., Cechetto, J.D., Eltis, L.D., Brown, E.D., 2004. High-throughput screening identifies inhibitors of the SARS coronavirus main proteinase. Chem. Biol. 11 (10), 1445–1453.

Buker, S.M., Gurard-Levin, Z.A., Wheeler, B.D., Scholle, M.D., Case, A.W., Hirsch, J.L., Ribich, S., Copeland, R.A., Boriack-Sjodin, P.A., 2020. A mass spectrometric assay of METTL3/METTL14 methyltransferase activity. SLAS Discov 25 (4), 361–371.

Coronaviridae Study Group of the International Committee on Taxonomy of V, 2020. The species Severe acute respiratory syndrome-related coronavirus: classifying 2019-nCoV and naming it SARS-CoV-2. Nat Microbiol 5 (4), 536–544.

Dai, W., Zhang, B., Su, H., Li, J., Zhao, Y., Xie, X., Jin, Z., Liu, F., Li, C., Li, Y., Bai, F., Wang, H., Cheng, X., Cen, X., Hu, S., Yang, X., Wang, J., Liu, X., Xiao, G., Jiang, H., Rao, Z., Zhang, L.K., Xu, Y., Yang, H., Liu, H., 2020. Structure-based design of antiviral drug candidates targeting the SARS-CoV-2 main protease. Science. https://doi.org/10.1126/science.abb4489.

Fan, K., Ma, L., Han, X., Liang, H., Wei, P., Liu, Y., Lai, L., 2005. The substrate specificity of SARS coronavirus 3C-like proteinase. Biochem. Biophys. Res. Commun. 329 (3), 934–940.

Gao, D., Hiromura, M., Yasui, H., Sakurai, H., 2002. Direct reaction between shikonin and thiols induces apoptosis in HL60 cells. Biol. Pharm. Bull. 25 (7), 827–832.

Grum-Tokars, V., Ratia, K., Begaye, A., Baker, S.C., Mesecar, A.D., 2008. Evaluating the 3C-like protease activity of SARS-Coronavirus: recommendations for standardized assays for drug discovery. Virus Res. 133 (1), 63–73.

Gurard-Levin, Z.A., Scholle, M.D., Eisenberg, A.H., Mrksich, M., 2011. High-throughput screening of small molecule libraries using SAMDI mass spectrometry. ACS Comb. Sci. 13 (4), 347–350.

Harapan, H., Itoh, N., Yufika, A., Winardi, W., Keam, S., Te, H., Megawati, D., Hayati, Z., Wagner, A.L., Mudatsir, M., 2020. Coronavirus disease 2019 (COVID-19): a literature review. J Infect Public Health 13 (5), 667–673.

Ison, M.G., Wolfe, C., Boucher, H.W., 2020. Emergency use authorization of remdesivir: the need for a transparent distribution process. J. Am. Med. Assoc. https://doi.org/10.1001/jama.2020.8863.

Ivens, T., Van den Eynde, C., Van Acker, K., Nijs, E., Dams, G., Bettens, E., Ohagen, A., Pauwels, R., Hertogs, K., 2005. Development of a homogeneous screening assay for automated detection of antiviral agents active against severe acute respiratory syndrome-associated coronavirus. J. Virol Methods 129 (1), 56–63.

Jin, Z., Du, X., Xu, Y., Deng, Y., Liu, M., Zhao, Y., Zhang, B., Li, X., Zhang, L., Peng, C., Duan, Y., Yu, J., Wang, L., Yang, K., Liu, F., Jiang, R., Yang, X., You, T., Liu, X., Yang, X., Bai, F., Liu, H., Liu, X., Guddat, L.W., Xu, W., Xiao, G., Qin, C., Shi, Z., Jiang, H., Rao, Z., Yang, H., 2020. Structure of M(pro) from SARS-CoV-2 and discovery of its inhibitors. Nature 582 (7811), 289–293. https://doi.org/10.1038/s41586-020-2223-y.

Jochmans, D., Leyssen, P., Neyts, J., 2012. A novel method for high-throughput screening to quantify antiviral activity against viruses that induce limited CPE. J. Virol Methods 183 (2), 176–179.

Kaeberlein, M., McDonagh, T., Heltweg, B., Hixon, J., Westman, E.A., Caldwell, S.D., Napper, A., Curtis, R., DiStefano, P.S., Fields, S., Bedalov, A., Kennedy, B.K., 2005. Substrate-specific activation of sirtuins by resveratrol. J. Biol. Chem. 280 (17), 17038–17045.

Kim, Y., Liu, H., Galasiti Kankanamalage, A.C., Weerasekara, S., Hua, D.H., Groutas, W. C., Chang, K.O., Pedersen, N.C., 2016. Reversal of the progression of fatal coronavirus infection in cats by a broad-spectrum coronavirus protease inhibitor. PLoS Pathog. 12 (3), e1005531.

Kim, Y., Lovell, S., Tiew, K.C., Mandadapu, S.R., Alliston, K.R., Battaile, K.P., Groutas, W. C., Chang, K.O., 2012. Broad-spectrum antivirals against 3C or 3C-like proteases of picornaviruses, noroviruses, and coronaviruses. J. Virol. 86 (21), 11754–11762.

Kuang, W.F., Chow, L.P., Wu, M.H., Hwang, L.H., 2005. Mutational and inhibitive analysis of SARS coronavirus 3C-like protease by fluorescence resonance energy transfer-based assays. Biochem. Biophys. Res. Commun. 331 (4), 1554–1559.

Lee, H., Torres, J., Truong, L., Chaudhuri, R., Mittal, A., Johnson, M.E., 2012. Reducing agents affect inhibitory activities of compounds: results from multiple drug targets. Anal. Biochem. 423 (1), 46–53.

Liu, Y., Kati, W., Chen, C.M., Tripathi, R., Molla, A., Kohlbrenner, W., 1999. Use of a fluorescence plate reader for measuring kinetic parameters with inner filter effect correction. Anal. Biochem. 267 (2), 331–335.

Liu, Y.C., Huang, V., Chao, T.C., Hsiao, C.D., Lin, A., Chang, M.F., Chow, L.P., 2005. Screening of drugs by FRET analysis identifies inhibitors of SARS-CoV 3CL protease. Biochem. Biophys. Res. Commun. 333 (1), 194–199.

Ma, C., Sacco, M.D., Hurst, B., Townsend, J.A., Hu, Y., Szeto, T., Zhang, X., Tarbet, B., Marty, M.T., Chen, Y., Wang, J., 2020. Boceprevir, GC-376, and calpain inhibitors II, XII inhibit SARS-CoV-2 viral replication by targeting the viral main protease. Cell Res. 30, 678–692.

Min, D.H., Tang, W.J., Mrksich, M., 2004. Chemical screening by mass spectrometry to identify inhibitors of anthrax lethal factor. Nat. Biotechnol. 22 (6), 717–723.

Mizumoto, K., Kagaya, K., Zarebski, A., Chowell, G., 2020. Estimating the asymptomatic proportion of coronavirus disease 2019 (COVID-19) cases on board the Diamond Princess cruise ship, Yokohama, Japan. Euro Surveill. 25 (10), 2020.

Mrksich, M., 2008. Mass spectrometry of self-assembled monolayers: a new tool for molecular surface science. ACS Nano 2 (1), 7–18.

O'Kane, P.T., Dudley, Q.M., McMillan, A.K., Jewett, M.C., Mrksich, M., 2019. High-throughput mapping of CoA metabolites by SAMDI-MS to optimize the cell-free biosynthesis of HMG-CoA. Sci Adv 5 (6), eaaw9180.

Palmier, M.O., Van Doren, S.R., 2007. Rapid determination of enzyme kinetics from fluorescence: overcoming the inner filter effect. Anal. Biochem. 371 (1), 43–51.

Patel, K., Sherrill, J., Mrksich, M., Scholle, M.D., 2015. Discovery of SIRT3 inhibitors using SAMDI mass spectrometry. J. Biomol. Screen 20 (7), 842–848.

Pedersen, N.C., Kim, Y., Liu, H., Galasiti Kankanamalage, A.C., Eckstrand, C., Groutas, W. C., Bannasch, M., Meadows, J.M., Chang, K.O., 2018. Efficacy of a 3C-like protease inhibitor in treating various forms of acquired feline infectious peritonitis. J. Feline Med. Surg. 20 (4), 378–392.

Rodriguez, C.E., Fukuto, J.M., Taguchi, K., Froines, J., Cho, A.K., 2005. The interactions of 9,10-phenanthrenequinone with glyceraldehyde-3-phosphate dehydrogenase (GAPDH), a potential site for toxic actions. Chem. Biol. Interact. 155 (1–2), 97–110.

Shen, M.L., Lipsky, J.J., Naylor, S., 2000. Role of disulfiram in the in vitro inhibition of rat liver mitochondrial aldehyde dehydrogenase. Biochem. Pharmacol. 60 (7), 947–953.

Swalm, B.M., Knutson, S.K., Warholic, N.M., Jin, L., Kuntz, K.W., Keilhack, H., Smith, J. J., Pollock, R.M., Moyer, M.P., Scott, M.P., Copeland, R.A., Wigle, T.J., 2014. Reaction coupling between wild-type and disease-associated mutant EZH2. ACS Chem. Biol. 9 (11), 2459–2464.

Szymczak, L.C., Huang, C.F., Berns, E.J., Mrksich, M., 2018. Combining SAMDI mass spectrometry and peptide arrays to profile phosphatase activities. Methods Enzymol. 607, 389–403.
Takahashi, D., Kim, Y., Lovell, S., Prakash, O., Groutas, W.C., Chang, K.O., 2013. Structural and inhibitor studies of norovirus 3C-like proteases. Virus Res. 178 (2), 437–444.
Valente, C., Moreira, R., Guedes, R.C., Iley, J., Jaffar, M., Douglas, K.T., 2007. The 1,4-naphthoquinone scaffold in the design of cysteine protease inhibitors. Bioorg. Med. Chem. 15 (15), 5340–5350.
Wiench, B., Eichhorn, T., Paulsen, M., Efferth, T., 2012. Shikonin directly targets mitochondria and causes mitochondrial dysfunction in cancer cells. Evid Based Complement Alternat Med 726025, 2012.
Wigle, T.J., Swinger, K.K., Campbell, J.E., Scholle, M.D., Sherrill, J., Admirand, E.A., Boriack-Sjodin, P.A., Kuntz, K.W., Chesworth, R., Moyer, M.P., Scott, M.P., Copeland, R.A., 2015. A high-throughput mass spectrometry assay coupled with redox activity testing reduces artifacts and false positives in lysine demethylase screening. J. Biomol. Screen 20 (6), 810–820.
Zauner, T., Berger-Hoffmann, R., Muller, K., Hoffmann, R., Zuchner, T., 2011. Highly adaptable and sensitive protease assay based on fluorescence resonance energy transfer. Anal. Chem. 83 (19), 7356–7363.
Zhang, L., Lin, D., Sun, X., Curth, U., Drosten, C., Sauerhering, L., Becker, S., Rox, K., Hilgenfeld, R., 2020. Crystal structure of SARS-CoV-2 main protease provides a basis for design of improved alpha-ketoamide inhibitors. Science 368 (6489), 409–412.
Zhou, H., Fang, Y., Xu, T., Ni, W.J., Shen, A.Z., Meng, X.M., 2020. Potential therapeutic targets and promising drugs for combating SARS-CoV-2. Br. J. Pharmacol. 177 (14), 3147–3161.
Zorman, J., Susjan, P., Hafner-Bratkovic, I., 2016. Shikonin suppresses NLRP3 and AIM2 inflammasomes by direct inhibition of caspase-1. PloS One 11 (7), e0159826.